Enhanced effects of curcumin encapsulated in polycaprolactone-grafted oligocarrageenan nanomicelles, a novel nanoparticle drug delivery system

Latufa Youssouf, Archana Bhaw-Luximon, Nicolas Diotel, Aurélie Catan, Pierre Giraud, Fanny Gimié, Dimitri Koshel, Sandra Casale, Sébastien Bénard, Vincent Meneyrol, et al.

Enhanced effects of curcumin encapsulated in polycaprolactone-grafted oligocarrageenan nanomicelles, a novel nanoparticle drug delivery system

Latufa Youssouf [a], Archana Bhaw-Luximon [b], Nicolas Diotel [a], Aurélie Catan [a], Pierre Giraud [a], Fanny Gimié [c], Dimitri Koshel [c], Sandra Casale [d], Sébastien Bénard [c], Vincent Meneyrol [c], Laura Lallemand [c], Olivier Meilhac [a,e] , Christian Lefebvre D'Hellencourt [a], Dhanjay Jhurry [b] and Joël Couprie [a, *]

[a]*Université de La Réunion, INSERM, UMR 1188 Diabète athérothrombose Thérapies Réunion Océan Indien (DéTROI), 97490 Saint-Denis de La Réunion, France*

[b]*Biomaterials, Drug Delivery and Nanotechnology Unit, Centre for Biomedical and Biomaterials Research (CBBR), University of Mauritius, MSIRI Building, Réduit, Mauritius*

[c] *Plateforme de recherche CYROI, 2 rue Maxime Rivière, 97490 Sainte-Clotilde, La Réunion, France*

[d]*Université Pierre et Marie Curie, Institut des Matériaux Paris Centre IMPC – FR2482 Tour 43/44 - 3ème étage - Pièce 320 - 4, place Jussieu 75252 Paris cedex 05, France*

[e] *Centre d'Investigation Clinique, CHU de La Réunion, 97448 Saint-Pierre, Réunion, France*

[*] Corresponding author. Tel.: +262 692 22 23 88; Fax: +262 262 93 82 37; *UMR DéTROI, 2 rue Maxime Rivière, 97490 SAINTE CLOTILDE, La Réunion, France. E-mail address*: joel.couprie@univ-reunion.fr

Abstract

One of the most effective strategies to enhance the bioavailability and the therapeutic effect of hydrophobic drugs is the use of nanocarriers. We have used κ-carrageenan extracted from *Kappaphycus alvarezii* to produce oligocarrageenan via an enzymatic degradation process. Polycaprolactone (PCL) chains were grafted onto the oligocarrageenans using a protection/deprotection technique yielding polycaprolactone-grafted oligocarrageenan. The resulting amphiphilic copolymers formed spherical nanomicelles with a mean size of 187 ± 21 nm. Hydrophobic drugs such as curcumin were efficiently encapsulated in the micelles and released within 24 to 72 h in solution. The micelles were non-cytotoxic and facilitated the uptake of curcumin by endothelial EA-hy926 cells. They also increased the anti-inflammatory effect of curcumin in TNF-alpha-induced inflammation experiments. Finally, *in vivo* experiments supported a lack of toxicity in zebrafish and thus the potential use of

polycaprolactone-grafted oligocarrageenan to improve the delivery of hydrophobic compounds to different organs, including liver, lung and brain as shown in mice.

Keywords: graft-copolymer; curcumin; nanomicelles; drug delivery; inflammation; endothelial cells

1. Introduction

It is known that the therapeutic effect of most hydrophobic drugs is lowered due to poor bioavailability (Savjani, Gajjar, & Savjani, 2012; Xu, Ling, & Zhang, 2013). Nanocarriers improve drug efficiency by enhancing their solubility and biodistribution (Shakeel, Ramadan, & Shafiq, 2009). Natural polymer-based nanoparticles such as polysaccharides are favoured due to their nontoxic properties, biodegradability, biocompatible nature and high hydroxyl content allowing further functionalization. Polysaccharides such as oligoagarose, chitosan and alginates from seaweeds have been used to engineer drug delivery devices which have shown sustained release (Bhaw-Luximon, Meeram, Jugdawa, Helbert, & Jhurry, 2011; Cook, Tzortzis, Charalampopoulos, & Khutoryanskiy, 2011; Nesamony, Singh, Nada, Shah, & Kolling, 2012; Cavalli, Leone, Minelli, Fantozzi, & Dianzani, 2014).

Although, marine polysaccharides are mostly used in the food and cosmetics industries, they are largely present in pharmaceutical applications, with an increasing interest in their use as materials for the incorporation of bioactive agents (Cardoso,Pereira, Seca, Pinto, & Silva,.2015). Furthermore, seaweed polysaccharides have been shown to have enormous potential in the biomedical field (Venkatesan et al., 2015). Amongst them, sulphated polysaccharides represent a group of major interest for their bioactivities resulting from their numerous hydroxyl groups which can act as recognition sites for cells and also from the backbone of their repeat unit which resembles *in vivo* polysaccharides such as hyaluronic acid. Their bioactivities include antioxidant (Barahona, Chandía, Encinas, Matsuhiro, & Zúñiga, 2011), anticoagulant (Ciancia, Quintana, & Cerezo, 2010), anticancer (Boopathy & Kandasamy, 2010), antiviral (Bouhlal et al., 2011), anti-allergic (Sang, Ngo, & Kim, 2012) and anti-inflammatory properties (Cumashi et al., 2007).

Carrageenan, a sulphated marine polysaccharide from red seaweeds, has been explored for its use as a source for sustained drug delivery nanoparticles. Depending on their degree of sulfation, the position of the sulfate group and the presence of 3-6-anhydro bridges,

carrageenans are classified into different families, the three main ones being kappa (κ), iota (ι) and lambda (λ) carrageenans (Figure S1a). The use of carrageenans as drug delivery carriers in the form of carrageenan-based pellets, beads, nanoparticles, microparticles, hydrogels, films and matrices has been investigated (Cunha & Grenha, 2016). A major advantage of polysaccharides including carrageenan is the presence of numerous hydroxyl groups that can be chemically modified to modulate their properties or to target specific cells for drug delivery applications. However, the insolubility of high molar mass carrageenans in common solvents and water renders their functionalization difficult. Some of us previously reported on the enzymatic degradation of another marine polysaccharide, namely agarose, into oligoagarose which was then transformed into oligoagarose-g-polycaprolactone amphiphilic micelles and showed drug delivery abilities in preliminary studies with a model molecule, ketoprofen (Bhaw-Luximon et al., 2011). Controlled grafting of polycaprolactone chains was achieved through partial protection-deprotection of the hydroxyl groups on oligoagarose and ring-opening polymerization of ε-caprolactone. Chitosan-graft-poly(ε-caprolactone) amphiphilic copolymer micelles have also been reported for 5-fluorouracil (5-FU) drug delivery with a release half-time up to 54.46 h and 5-FU comparable cytotoxic effect in A549 cells. (Gu, Le, Lang, & Liu, 2014). Recently, cyclodextrin-g-polyurethane has been prepared using NCO-terminated polyurethane of MW 1400, grafted on cyclodextrin via its hydroxyl groups. The graft copolymer showed sustained release of dexamethasone (40-56%) over 42 h compared to 100% release within 2 hours with cyclodextrin alone. This system also showed sustained cytotoxic effects on HeLa cells, inducing from 25 to 75% mortality over 72 h. Thus, grafted polysaccharides can be explored as amphiphilic micelles with a hydrophobic core for drug encapsulation.

Curcumin (diferuloylmethane) is the main curcuminoid present in turmeric (Figure S1b). This molecule possesses significant anti-inflammatory, antioxidant, anti-carcinogenic, anti-mutagenic, anticoagulant, and anti-infective effects (Mahmood, Zia, Zuber, Salman, & Anjum, 2015). Curcumin also exerts a protective effect against cardiovascular diseases, including atherosclerosis, mainly *via* diverse mechanisms including inhibition of oxidative stress, inflammation, and cell death (He et al., 2015). However, due to its hydrophobic nature, its rapid metabolism and its physicochemical and biological instability, curcumin has a poor bioavailability. To circumvent these difficulties, several approaches have been proposed such as encapsulation in liposomes and polymeric micelles, inclusion complex formation with cyclodextrin or formation of polymer–curcumin conjugates (Mahmood et al., 2015).

We previously published a new process to extract alginates from brown seaweeds (*Sargassum binderi* and *Turbinaria ornata*) and carrageenans from red seaweeds (*Kappaphycus alvarezii* and *Euchema denticulatum*) using ultrasound (Youssouf et al., 2017). In this paper, we report production of the enzymatically-modified κ-carrageenan to produce oligocarrageenan that was then grafted with polycaprolactone chains in order to form spherical nanomicelles allowing vectorization of hydrophobic molecules such as curcumin. The micelles were characterized using Dynamic Light Scattering (DLS) and Scanning and Transmission Electron Microscopy (SEM and TEM). We discuss here the effect of the curcumin-loaded nanomicelles on vascular endothelial cells, EA-hy926, as well as their *in vivo* toxicity tested in zebrafish and the biodistribution of the nanomicelles in mice.

2. Materials and Methods

2.1. Materials

Carrageenans were extracted from cultivated red algae *Kappaphycus Alvarezii* received from Ibis Algoculture (Madagascar) as described previously (Youssouf et al., 2017). *Pseudoaltermonas carrageenovora* bacteria were obtained from DSMZ, Germany. For the PCL grafting on carrageenan, all chemical products were purchased from Sigma-Aldrich. D_2O or $CDCl_3$ used for NMR analysis were from Eurisotop (France).

Curcumin was synthesized according to the method previously reported by Pedersen et al. (Pedersen, Rasmussen, & Lawesson, 1985). The chromatogram and the NMR spectrum of the product are presented in Figures S2 and S3.

The human endothelial cell line, EA-hy926, was obtained from ATCC and cultured in a Dulbecco's Modified Eagle Medium (DMEM) supplemented with 10% heat-inactivated Fetal Bovine Serum (FBS), 100 units penicillin/mL, 100 µg streptomycin/mL and HAT (hypoxanthine 100 µM; aminopterin 0.4 µM and thymidine 16 µM) at 37 °C in a 5% CO_2 humidified atmosphere.

Three to six months-old adult male and female wild type zebrafish (*Danio rerio*) were purchased from commercial suppliers and maintained under standard conditions of photoperiod (14/10 h light/dark), temperature (28 °C) and oxygenation. They were fed daily with commercially available dry food (TetraMin).

C57Bl6 mice used to study the biodistribution of injected molecules, were purchased from Charles River Laboratories (Saint-Germain-sur-L'Arbresles, France). C57Bl6 mice were maintained at a constant temperature (23±1 °C) and a hygrometry between 55 to 65% under a 12-hour light/dark cycle, were permitted free access to food and water and were handled and cared in accordance with guidelines for care and use of laboratory animals of the European Council Directive 2010/63/EU approved by the Ethics Committee of La Reunion, n°114, for Animal Experimentation under the reference APAFIS#9119-2016090515329223v2.

2.2. Extraction of κ-carrageenan from *Kappaphycus Alvarezii*

To extract carrageenan, algae were first pre-treated with a hydro-alcoholic solution (80% ethanol), and carrageenans were then extracted in hot water (90 °C, pH 7) with ultrasonication (150 W, 15 min). Afterwards, a hot filtration was performed to remove algae residues. Carrageenans were then jellified by lowering the temperature to 4 °C, isolated by filtration, frozen and lyophilized. The resulting carrageenans were composed of κ-carrageenan (68%) and λ-carrageenan (32%) as evidenced by NMR (Youssouf et al., 2017).

2.3. Production and isolation of κ-carrageenase from *P. carrageenovora*

κ-carrageenase was expressed and isolated from *Pseudoaltermonas carrageenovora* after stimulation with a κ-carrageenan solution. The protocol was adapted from that used for the production of λ-carrageenan from the same bacterial strain (Guibet et al., 2007). Bacteria were grown in 1 liter of Marine Broth culture medium in Erlen flasks incubated at 21 °C under shaking. After 3 to 4 h of culture, when the OD_{600nm} reached 0.6, the expression of κ-carrageenase was stimulated with a stock solution of κ-carrageenan dissolved in Tris-HCl 100 mM pH=8.5 at a final κ-carrageenan concentration of 0.15% (Mass/Volume of culture). After 24 h of culture, bacteria were eliminated by centrifugation (3000 g, 30 min, 4 °C). The supernatant was filtered first through a 0.45 µm filter and then through a 300 kDa membrane. The enzyme was then concentrated using a 10 kDa centrifugal filter and desalting was performed with a 3 kDa centrifugal filter. The protein content was determined using the Bradford assay.

Enzymatic digestion was carried out to obtain oligocarrageenans using κ-carrageenase isolated from *Pseudoaltermonas carrageenovora*. 150 mg of carrageenans were dissolved in a tris-HCl solution (100 mM, pH 8.5) and incubated with κ-carrageenase (75.3 µg in 1 mL). Different durations of digestion (2 h, 6 h and 24 h) were tested. An ultrafiltration using a 10 kDa centricon device was then performed to eliminate the enzyme, non-hydrolysed κ-carrageenan and λ-carrageenan. Oligocarrageenans were then isolated by precipitation with

methanol and the product was freeze-dried and analysed by NMR and Size Exclusion Chromatography (SEC).

The enzymatic activity was evaluated by measuring the amount of reducing sugar according to the assay described by Kidby and Davidson (Kidby & Davidson, 1973). After hydrolysis, 100 µL of substrate were mixed with 900 µL of ferricyanide solution 1X (300 mg potassium hexacyanoferrate III, 28 g of Na_2CO_3, 1 mL NaOH 5 M *QS* 1 L). The mixture was boiled for 10 min and the absorbance at 420 nm was measured at room temperature. The control was obtained in the same condition by using a boiled-inactivated enzyme. The method was calibrated using a glucose solution ranging from 0 to 300 µg. mL^{-1}.

2.4. Synthesis of polycaprolactone-grafted oligocarrageenan

The synthesis of polycaprolactone-grafted oligocarrageenan involved three steps: (i) partial acetylation of the hydroxyl groups on oligocarrageenan; (ii) polymerisation of caprolactone on the partially acetylated oligocarrageenan; (iii) deprotection of the hydroxyl groups. The protocol was adapted from a previous study in which polycaprolactone was grafted onto oligoagarose (Bhaw-Luximon et al., 2009).

(i) Partial acetylation of oligocarrageenan

4 mL of pyridine and 644 µL of acetic anhydride were added to 500 mg of oligocarrageenan. The mixture was placed at room temperature under stirring for 3 h. The reaction was stopped by adding ice to the mixture to hydrolyse unreacted acetic anhydride and partially acetylated-oligocarrageenans were isolated by precipitation using cold methanol. The precipitate was then frozen, lyophilized and characterized by NMR.

(ii) Polymerization of caprolactone

To graft hydrophobic chains onto the oligomers, 200 mg of acetylated-oligocarrageenan were dissolved in 2 mL of toluene and 20 µL of the catalyst tin (II) ethylhexanoate was added. After 2 h of stirring at 40 °C under a nitrogen atmosphere, 330 mg of ε-caprolactone were added and polymerization was allowed to proceed for 20 h at 110 °C. The stability of partially acetylated oligocarrageenan and the absence of depolymerisation in these conditions was confirmed by Thermal Gravimetric Analysis (TGA), Differential Scanning Calorimetry (DSC) and NMR analyses (data not shown). The resulting acetylated-OligoKC-g-PCL was dissolved in chloroform and precipitated in cold methanol. After freezing and lyophilization, the product was characterized by NMR.

196 *(iii) Deprotection of hydroxyl groups from* polycaprolactone-grafted acetylated-
197 oligocarrageenan

198 To remove acetyl groups from polycaprolactone-grafted acetylated-oligocarrageenan, the
199 copolymer was dissolved in a solution of THF/methanol (v/v=1/1). A sodium methoxide
200 ($NaOCH_3$) solution was added drop by drop to reach pH 8 and the mixture was kept under
201 stirring at room temperature. After 4 h, the solution was neutralized with 0.5 M HCl and then
202 underwent vacuum evaporation. The product was resuspended in water under stirring for 1 h.
203 Precipitated PCL was eliminated through a 0.22 µm filter and unreacted caprolactone was
204 removed by dialysis through a 2 kDa membrane. In water, the amphiphilic copolymers,
205 named polycaprolactone-grafted oligocarrageenan, become soluble by forming micelles. The
206 product was freeze-dried and then analyzed by NMR.

207 2.5. NMR analysis

208 All NMR analyses were performed on a 600 MHz Avance III Bruker NMR spectrometer
209 equipped with a $^{1}H/^{19}F$, ^{13}C and ^{15}N cryoprobe. 1D ^{1}H, 1D ^{13}C, 2D COSY and 2D ^{1}H-^{13}C
210 HSQC spectra were recorded in 100% D_2O or $CDCl_3$ at room temperature and
211 tetramethylsilane was used as reference. ^{1}H NMR spectra were recorded with 128 scans using
212 a sweep width of 10 ppm. 2D spectra were obtained with 32 scans and a sweep width of 10
213 ppm for ^{1}H and 120 ppm for ^{13}C. In all spectra, the carrier was placed at 4.7 ppm for ^{1}H and
214 50 ppm for ^{13}C.

215 2.6. Size exclusion chromatography

216 Size Exclusion Chromatography (SEC) was performed on a 1260 Infinity GPC/SEC
217 System (Agilent Technologies) with a PSS Suprema column. The sample was passed through
218 a 0.22 µm filter and 400 µL of the solution (1 mg/mL) was injected onto the column. Elution
219 was carried out at a flow rate of 1 mL/min with a 0.5 g/l $NaNO_3$ solution. A calibration curve
220 was obtained using a mixture of dextrans of various molar weights (180 Da, 4400 Da, 21400
221 Da and 277 000 Da).

222 2.7. Drug loading - Acetone volatilization method

223 Encapsulation of curcumin, rifampicin and Nile Red was performed using the acetone
224 volatilization method. Typically, 500 mg of polycaprolactone-grafted oligocarrageenan and
225 50 mg of drug were dissolved in 10 mL of acetone. Deionized water was added slowly
226 dropwise (250 mL) and the mixture was kept under stirring at room temperature overnight.
227 Acetone was then evaporated at 30 °C and the precipitate corresponding to the non-
228 encapsulated drug was eliminated by passage through a 0.22 µm filter. Dialysis was

performed using a membrane with a MWCO of 2000 Da to remove free drugs. Nanomicelles loaded with curcumin, rifampicin or Nile Red were lyophilized. The amount of encapsulated curcumin was determined by fluorescence measurements (Nile Red, excitation wavelength = 550 nm – emission wavelength = 630 nm), or by absorbance (at 420 nm for curcumin and 475 nm for rifampicin).

2.8. *In vitro* release of encapsulated drug

10 mg of drug-loaded micelles were dissolved in 5 mL of PBS and subjected to dialysis at 37 °C using a Cellu-Sep H1 dialysis membrane (MWCO = 2000 Da) immersed in 100 mL of PBS. The amount of drug released into the external medium was measured either by fluorescence (excitation wavelength = 550 nm; emission wavelength = 630 nm for Nile Red), or by absorbance (at 420 nm for curcumin and 475 nm for rifampicin) over 3 days.

2.9. Determination of morphology and particle size

The particle size and distribution of micelles were recorded on a Dynamic Light Scattering (DLS) particle size analyzer (90 Plus Particle Size Analyzer, Dynamic Light Scattering (Brookhaven Instruments Corporation) or a Zetasizer Nano (Malvern Instruments). The analyses were conducted in aqueous solution after filtration through a 0.22 µm filter to remove free drug/small polymer aggregates. Each analysis was performed at 25 °C in triplicate with an angle detection of 90°. The CMC (Critical Micelle concentration) was determined by DLS analysis of polycaprolactone-grafted oligocarrageenan dissolved in H_2O at concentrations ranging from 0.2 to 2 mg/mL. To obtain the CMC, the logarithm of intensity of the scattered light was plotted as a function of polycaprolactone-grafted oligocarrageenan concentration. The resulting plot can be fitted to two straight lines whose intercept corresponds to the CMC (Topel, Cakir, Budama, & Hoda, 2013 – Figure S4). The morphology of NPs was also examined by transmission electron microscopy (TEM) using a JEOL-1011 TEM instrument (tungsten filament) 100 kV. For TEM measurements, a drop of the nanoparticle solution was placed on a 10 nm thick carbon-coated copper grid. To obtain scanning electron microscopy (SEM) images, samples were mounted on aluminium studs and sputter-coated with gold/palladium for 120 s. To obtain scanning electron microscopy (SEM) images, samples were mounted on aluminium studs and sputter-coated with gold/palladium for 120 s. The micelles were then imaged by a TESCAN VEGA 3 LMU field emission scanning electron microscope at 10.0 kV.

2.10. Cytotoxicity of loaded polycaprolactone-grafted oligocarrageenan micelles

Cell toxicity of curcumin-loaded and empty micelles was evaluated by the MTT assay using EA-hy96 endothelial cells. Cells were seeded in 96-well plates in 200 µL of complete medium to obtain a concentration of 50,000 cells per well and incubated at 37 °C for 24 h. The medium in each well was then removed and replaced with 200 µL of fresh medium containing either empty micelles, curcumin-loaded micelles or free curcumin. Free curcumin was dissolved in DMSO at concentrations ranging from 0 to 20 µM, empty micelles and curcumin-loaded micelles were diluted in culture medium at concentrations ranging from 0.1 µg/mL to 1000 µg/mL. After 48 h, the supernatant was removed and an MTT solution (100 µL, 0.5 mg/mL) was added to each well and the cells were incubated for 4 h at 37 °C. The supernatant was then eliminated and 100 µL of DMSO were added to each well to dissolve the formazan crystals. The absorbance at 570 nm was measured with a microplate reader (Tecan, Infinite M200Pro).

2.11. Cellular uptake of micelles by fluorescence microscopy

EA-hy926 cells were cultured to about 70% confluency in 12-well microplates containing cover slips with 2 mL of complete medium. After 24 h, the culture medium was replaced with fresh medium containing curcumin or curcumin-loaded micelles at a curcumin concentration of 15 µM and incubated at 37 °C for 4 h, 6 h, 8 h, 16 h or 24 h. After incubation, the culture medium was removed, and the cells were washed three times with PBS to remove micelles or free curcumin that were not incorporated into the cells. EA-hy926 cells were then fixed using 4% paraformaldehyde in PBS (10 min) at room temperature, incubated with DAPI (200 ng/mL) for 20 min at room temperature and visualized using an Eclipse 80i fluorescence microscope (Nikon, France) equipped with a Hamamatsu ORCA-ER digital camera (Life Sciences, Japan). Quantification was then performed by determining the mean curcumin fluorescence of 90 cells for each condition in three independent experiments using ImageJ software.

2.12. Quantification of TNF- α -induced secretion of IL-6 and MCP-1 by EA-hy926 cells

The protective effect of curcumin on EA-hy926 cells was evaluated. Cells were seeded in 6-well microplates containing 2 mL of culture medium and cultured to confluency (24 h). The medium was then replaced with solutions containing empty micelles, curcumin-loaded micelles or free curcumin respectively. Two concentrations of curcumin were tested, namely 5 µM and 15 µM. After 24 h, the medium was removed, and cells were stimulated with TNF-α (tumor necrosis factor-alpha) overnight, diluted in culture medium (200 µL, 10 ng/mL). The

supernatants were then subjected to ELISA (e.Biosciences, France) to measure the secretion of inflammatory factors (IL-6 and MCP-1). ELISA was performed according to the manufacturer's instructions.

2.13. Preliminary safety evaluation in zebrafish

To assess the *in vivo* toxicity of blank micelles, curcumin-loaded micelles and free curcumin, animals were injected intraperitoneally with these one of these respective solutions. Briefly, fish were deeply anesthetized with 0.02% tricaine and received a single intraperitoneal injection of blank micelles (300 mg/kg; n=12), free curcumin (195 µM; n=12), curcumin-loaded micelles (300 mg/kg equivalent to 195 µM of curcumin; n=12) or PBS (n=8). The viability of the three groups of zebrafish was then observed for 7 days. Zebrafish behaviour, stress and/or suffering were carefully monitored in order to eventually euthanize any suffering animals. No striking warning signs (stress, behavioural changes…) indicating that the treatments induced animal suffering were observed. All experiments were conducted in accordance with the French and European Community Guidelines for the Use of Animals in Research (86/609/EEC and 2010/63/EU) and approved by the local Ethics Committee for animal experimentation (APAFIS#9984-2016111814324578).

2.14. Biodistribution of free vs encapsulated Nile red in mice

Mice (12 weeks old, approximately 25 g) were randomly assigned to 1 of 2 groups (free Nile red and encapsulated Nile red): n=3 per group, 2 females and 1 male.

To study the biodistribution, free (225 µg) or encapsulated Nile red (100 mg/kg equivalent to 225 µg of Nile red) were injected via the tail vein using a 30-gauge catheter. Retro-orbital 140 µL blood sampling was performed 1 h, 2 h and 4 h after administration, under anaesthesia (isoflurane, 4% induction and 1.5% maintenance in air). Mice were then sacrificed and tissues (brain, liver, spleen, and kidney) were collected after perfusion with saline buffer. Nile Red was then extracted from tissues with a mixture of ethyl acetate/propanol (9:1) as described by Kim et al. (2011). Extracted Nile Red was then quantified by fluorescence (excitation wavelength = 550 nm – emission wavelength = 630 nm).

2.15. Statistical analysis

All statistical analyses were carried out using GraphPad Prism 5 software. Analysis of variance (ANOVA) was performed to compare all data. Significant differences were highlighted using a post-hoc Tukey test.

3. Results and Discussion

3.1 Synthesis of polycaprolactone-grafted oligocarrageenan

The synthesis of polycaprolactone-grafted oligocarrageenan was performed using a method described by Bhaw-Luximon et al., 2009. to obtain oligoagarose-graft-PCL starting from oligoagarose. Carrageenan was selectively degraded into oligocarrageenans using a κ-carrageenase enzyme isolated from *Pseudoaltermonas carrageenovora* followed by partial acetylation of the oligocarrageenan hydroxyl groups. The remaining free hydroxyl groups were then used to copolymerize ε-caprolactone. Finally, acetyl groups were removed to yield amphiphilic polycaprolactone-grafted oligocarrageenan which can self-assemble into micelles in aqueous solution.

Enzymatic degradation of κ-carrageenan to oligocarrageenan

κ-carrageenase (EC3.2.1.83) is a member of the glycoside hydrolase 16 family (GH16). This enzyme hydrolyses β-(1→4) linkage with retention of the anomeric configuration (Yao, Wang, Gao, Jin, & Wu, 2013; Knutsen et al., 2001; Sun et al., 2014). It can be isolated from the cell free culture medium of the bacteria *Pseudoaltermonas carrageenovora* (Guibet et al., 2007). κ-carrageenase was produced from a carrageenan-stimulated culture of *Pseudoaltermonas carrageenovora* and the enzyme was recovered from the bacterial culture medium. A reducing ends measurement was performed to check the activity of the enzyme (Figure S5A). The successful degradation can be measured by the increasing amount of reducing sugar during the degradation. The control reaction performed using boiled-inactivated enzyme showed no increase in reducing sugar level. Degradation products of κ-carrageenan were further characterized using gel permeation chromatography with a dextran calibration curve (Figure S5B). At 2 h, most of the κ-carrageenan was converted into octamers (DP8). After 24 h of degradation, hexamers (DP6) and dimers (corresponding to neo-κ-carrabiose) could be identified. A previous study on oligoagarose-*g*-polycaprolactone showed that oligosaccharide chains of between 8 and 15 repeat units were best suited for functionalization to form micelles (Bhaw-Luximon et al., 2009, 2011). Thus, to obtain a good yield of oligocarrageenan with DP8, hydrolysis of κ-carrageenan was performed for 6 h and oligocarrageenan was then separated from the enzyme and unreacted κ-carrageenan by ultrafiltration.

358 ***Acetylation of oligocarrageenan***

359 Partial acetylation of hydroxyl groups was performed with acetic anhydride in the presence
360 of pyridine at room temperature. The degree of acetylation was assessed using ^{1}H NMR using
361 the peak corresponding to the acetyl function at 2.13 ppm (Figure 1A). The degree of
362 acetylation was expected to be in the range 30-70% to obtain a good balance between the
363 hydrophilic oligocarrageenan chain and the hydrophobic PCL to be added in the next stage
364 (Bhaw-Luximon et al., 2009). ^{1}H NMR spectra indicated an acetylation of 60% using the
365 integration values of protons at 5.04 ppm and 4.6 ppm (corresponding to anomeric H in
366 oligocarrageenan) and at 2.13 ppm (acetyl groups).

367 ***Partially acetylated polycaprolactone-grafted oligocarrageenan***

368 Partially acetylated oligocarrageenan was used as a macroinitiator to polymerize ε-
369 caprolactone in the presence of tin(II) octanoate (Bhaw-Luximon et al., 2009). Different
370 lengths of polycaprolactone were obtained by varying the monomer to initiator ratio. ^{1}H
371 NMR spectra of the resulting products showed characteristic signals due to the PCL unit
372 (Figure 1B). Assignments of the polycaprolactone moiety were completed using information
373 from 1D ^{13}C, 2D COSY and ^{1}H-^{13}C HSQC spectra (Figure S6). The peaks at 3.99 and 2.23
374 ppm were assigned to -C**H**$_2$-O-C=O protons and -C**H**$_2$-C=O protons respectively. -C**H**$_2$-CH_2-
375 C**H**$_2$ proton groups were detected at 1.58 and CH_2-C**H**$_2$-CH_2 protons at 1.31 ppm. The NMR
376 spectra confirmed the expected copolymer structure. Copolymers with 10 caprolactone units
377 were selected for further studies.

378 ***Polycaprolactone-grafted oligocarrageenan***

379 Removal of acetyl groups was performed under mild conditions to avoid cleavage of the
380 grafted PCL chains. The ^{1}H NMR spectrum (Figure 1C) of the product showed PCL signals
381 between 1.3 and 4 ppm and oligocarrageenan signals from 3 to 5.5 ppm. The peak
382 corresponding to acetyl proton at 2.09 ppm was not detected after this last step indicating that
383 complete deprotection of hydroxyl groups was achieved. No change was found in the number
384 of caprolactone repeat units.

385

386

387

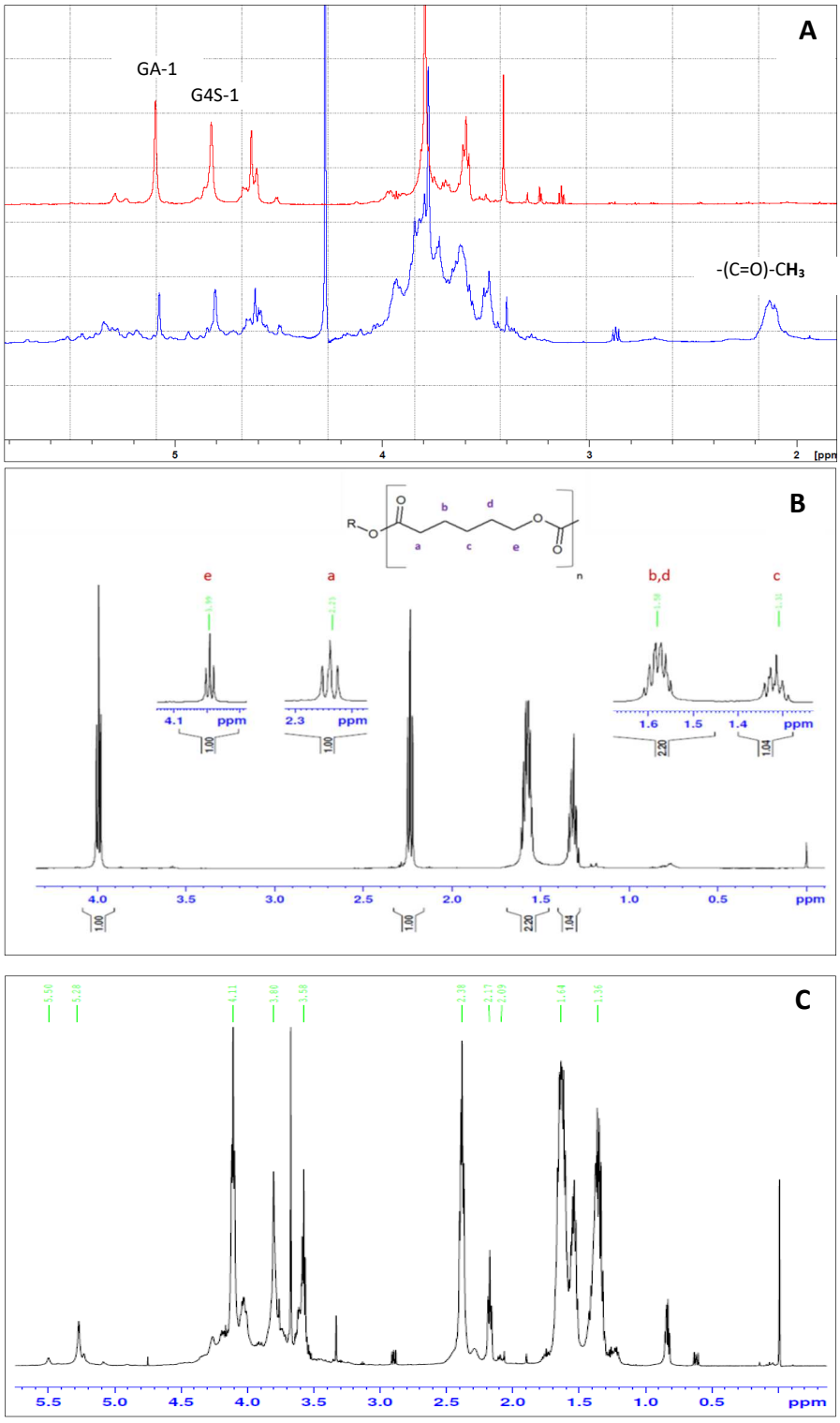

Figure 1: (A) ^{1}H NMR spectra of oligocarrageenan (red spectrum) and acetylated-oligocarrageenan (blue spectrum) obtained in D_2O. Acetyl-group protons were detected at 2.13 ppm. GA-1 and G4S correspond to anomeric protons of the repeat unit of κ-carrageenan. **(B)** ^{1}H NMR spectrum of acetylated-oligocarrageen-graft-PCL obtained in $CDCl_3$. a, b c, d and e correspond to caprolactone protons. R represent the partially acetylated-oligocarrageen chain. **(C)** ^{1}H NMR spectrum of oligocarrageen-graft-PCL obtained in D_2O. Signals corresponding to oligocarrageenan (between 3 ppm and 5.5 ppm) and caprolactone (between 1.3 ppm and 4 ppm) are both observed.

3.2 Characterization of micelles and drug loading-release

The amphiphilic copolymer self-assembled in water to form micelles with an average size of 187 ± 21 nm (Z-Average), as determined by dynamic light scattering (DLS) (Figure 2A.i). The CMC estimated by DLS was 4.10^{-5} M. This value was similar to that of $2.5.10^{-5}$ M of oligoagarose-*g*-PCL nanomicelles developed by Bhaw-Luximon et al. (2011).

TEM images of the micelles showed a spherical morphology with a diameter in the range of 100-150 nm (Figure 2B). The size of micelles appears generally smaller than the value determined by DLS, probably because of the dry state of samples in TEM measurements. This phenomenon has been reported by several other authors (Bordallo, Rieumont, Tiera, Gómez, & Lazzari, 2015; Wang et al., 2015). Similarly, a previous study on oligoagarose-graft-PCL resulted in a particle diameter of 20 nm by DLS and 12 nm by TEM (Bhaw-Luximon et al., 2011). SEM images also showed a uniform spherical morphology with a diameter in the range of 75-100 nm (Figure 2 C).

Encapsulation of hydrophobic molecules namely curcumin, rifampicin and Nile Red was performed using the acetone volatilisation method**.** After encapsulation a slight decrease in particle size was noted with a Z-Average value of 177,2 ± 1.2 nm (Figure 2A.ii). This could be explained by the high affinity between the hydrophobic micellar core and the hydrophobic molecule. The spherical nature of Nile red-loaded and curcumin-loaded micelles was confirmed by TEM and SEM images (Figure 2B and 2C).

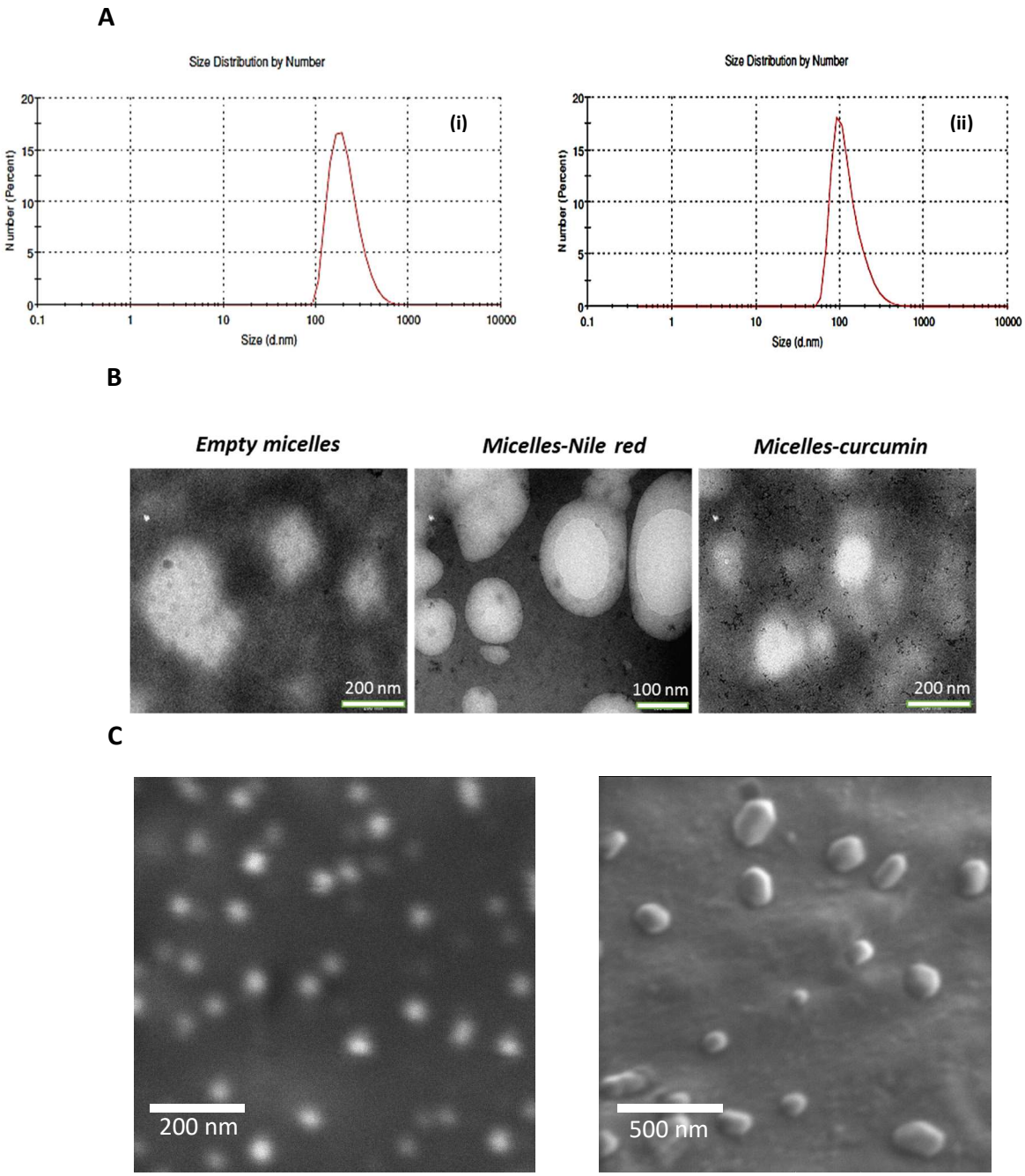

Figure 2: Characterization of oligocarrageenan-graft-PCL: (**A**) Size distribution of empty micelles (i) and curcumin-loaded micelles (ii) by Dynamic Light Scattering (DLS); (**B**) TEM images of empty micelles, Nile red loaded micelles and curcumin-loaded micelles at a concentration of 0.5 or 1 mg/mL; (**C**) SEM images of empty and curcumin loaded micelles.

Fluorescence analysis of curcumin showed a maximum emission at 558 nm for free curcumin and 517 nm for curcumin-loaded micelles (Figure 3A), which reflected the different chemical environments of curcumin. The encapsulation efficiency was determined using UV (curcumin, rifampicin) or fluorescence (Nile Red) measurements. A calibration curve allowed determination of the amount of encapsulated drug. The amount of encapsulated drug (w/w) was 10% for curcumin, 17% for rifampicin and 9% for Nile red.

The kinetics of hydrophobic molecule release from the micelles was studied in PBS at 37 °C (Figure 3B**).** Curcumin and Nile red were released over a longer period (with 65% released respectively after 72 and 60 h) than rifampicin which showed 70% release after 24 h. The time of release could depend on the affinity between the micelle core and the encapsulated molecule as shown previously by Jeetah et al. (Jeetah, Bhaw-Luximon, & Jhurry, 2013). The drug release probably proceeded via a combined erosion/diffusion mechanism due to the slow hydrolytic degradation rate of the polycaprolactone core. For instance, non-enzymatic degradation of PVP-b-PCL micelles is quite slow under neutral conditions and fast in acidic or basic media (Hu, Jiang, Chen, Wu, & Jiang, 2010).

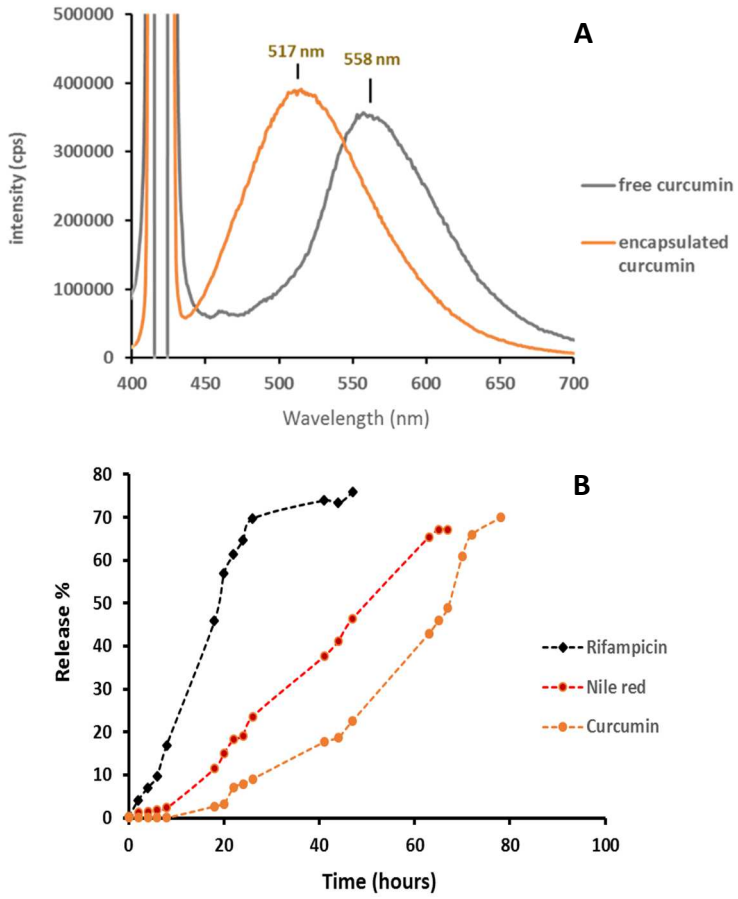

Figure 3: (**A**) Characterization of free curcumin and encapsulated curcumin by fluorescence. Excitation was performed at 420 nm, and the maximum emission wavelength of free curcumin and curcumin-loaded micelle was detected at 558 nm and 517 nm respectively. (**B**) Kinetics of release of curcumin, Nile red and rifampicin from OligoKC-g-PCL micelles. The concentrations of lipophilic molecule released in the medium during time was measured either by fluorescence (excitation wavelength = 550 nm – emission wavelength = 630 nm) for Nile Red, or by absorbance (at 420 nm for curcumin and 475 nm for rifampicin).

3.3. **Toxicity study of** polycaprolactone-grafted oligocarrageenan

To determine the relative toxicity of polycaprolactone-grafted oligocarrageenan on endothelial cells an MTT assay was used. Even if the MTT assay is not a direct measurement of viability, the quantification of mitochondrial activity is, in most cases, proportional to the number of cells and thus provides an indirect assessment of the toxicity. The empty micelles did not affect cell viability at concentrations up to 1000 µg/mL (Figure 4A). When the micelles were loaded with curcumin, cell viability was not affected up to a concentration of 250 µg/mL, corresponding to 67 µM of encapsulated curcumin. However, a significant decrease in viable cell number was observed at 500 µg/mL (Figure 4B). The cytotoxic effect of curcumin is well documented. Free curcumin at concentrations above 5 µM affected cell viability (Figure 4C) as previously described by Kam et al. (2015). Thus, curcumin-loaded polycaprolactone-grafted oligocarrageenan limited the cytotoxicity of curcumin. This could be explained by a progressive and sustained release of curcumin from the micelles. The MTT assay was performed after 48 h incubation whereas cell-free drug release kinetics indicated 23% release at 48 h (Figure 3 B) corresponding to an estimated released curcumin concentration of 16 µM at the highest non-cytotoxic micelle concentration (250 µg/mL micelle/curcumin). Both release kinetics and uptake of micelles may impact the bio-availability of intracellular curcumin. Furthermore, the cytotoxicity of released curcumin may be limited by cell biotransformation involving chemical or enzymatic processes (Heger, van Golen, Broekgaarden, & Michel, 2013).

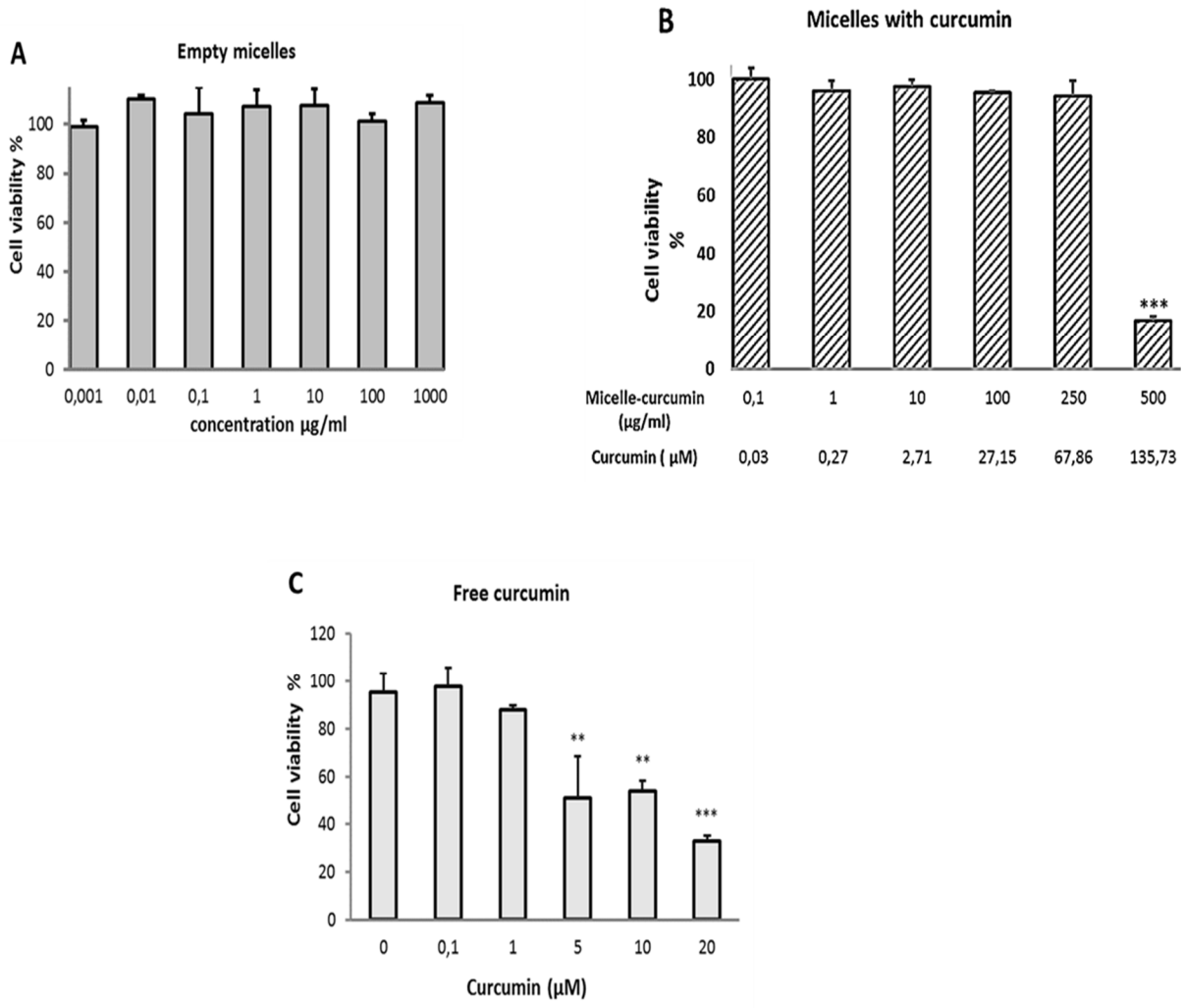

Figure 4: *In vitro* toxicity study of empty micelles and micelles loaded with curcumin. Cell viability of EA.hy926 cell was measured using MTT assay after treatment with empty micelles (**A**), curcumin-loaded micelles (**B**) or curcumin (**C**) for 48 h. *** ($p < 0.01$) significant difference compared with the control without treatment.

The zebrafish is well-recognized to be a suitable vertebrate model for toxicity assessment (Hill, Teraoka, Heideman, & Peterson, 2005; Nishimura et al., 2016). Consequently, we used zebrafish as an *in vivo* model to evaluate the acute toxicity of our nanomicelles (Figure 5). A previous study conducted in rats used intraperitoneal injection of curcumin (100 mg/kg to 300 mg/kg) and demonstrated beneficial effects of this polyphenol after stroke (Thiyagarajan & Sharma, 2004). We thus used a maximum concentration of 300 mg/kg of blank (vehicle) or curcumin-loaded micelles. After being deeply anesthetized, the fish were injected intraperitoneally with a single dose of empty micelles (300 mg/kg; n=12), curcumin-loaded micelles (300 mg/kg equivalent to 195 µM of curcumin; n=12), curcumin (5.5 mg/kg; 195 µM; n=12) or PBS (n=8). The viability of zebrafish was monitored over 7 days with no significant difference in survival rates

between the treated groups. Furthermore, the respective treatments did not result in any striking impairment of zebrafish behaviour, stress, locomotor activity or food intake.

Taken together, these results demonstrate the absence of visible toxic effects of the blank and curcumin-loaded micelles on the viability of adult zebrafish and on their main behaviour (stress, locomotor activity, and food intake) compared to PBS-injected ones. This reinforces the idea that polycaprolactone-grafted oligocarrageenan micelles are safe nanocarriers.

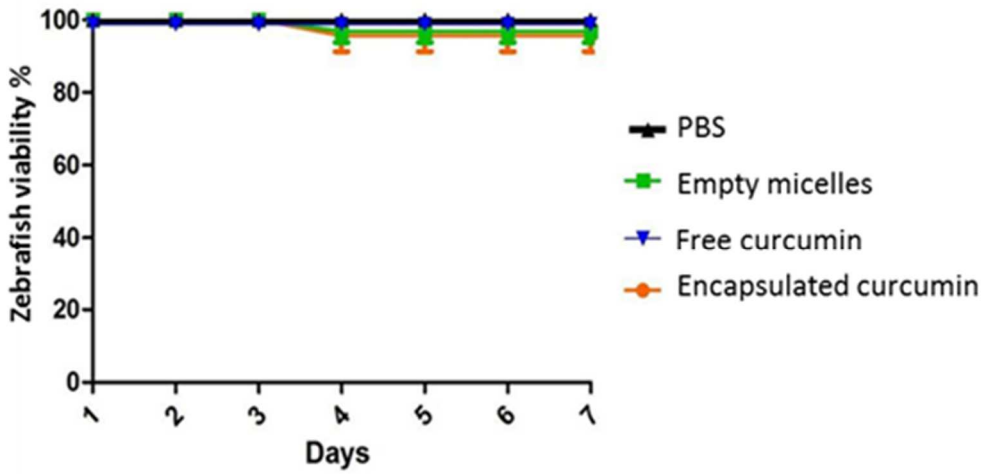

Figure 5: Effect of intraperitoneal injection of empty micelles (n=12), curcumin, encapsulated curcumin (n=12), Free curcumin (n=12) and PBS (n=8) on zebrafish viability. Zebrafish received an injection of 300 mg/kg of empty micelles, curcumin-loaded micelles, free curcumin or PBS and the viability was observed for 7 days, without any significant change between groups.

3.4. Cellular uptake of curcumin by EA.hy926 cells

The cellular uptake of OligoKC-g-PCL was investigated using endothelial EA-hy926 cells treated with free curcumin or curcumin-loaded micelles and stained with DAPI. As the treatment with free curcumin during 48 h showed a decrease in cell viability, the cell uptake kinetics were monitored from 4 h to 24 h. Treated cells were then visualized using fluorescence microscopy. Free curcumin could not be taken up effectively by the cells as demonstrated by low intensity of curcumin fluorescence (green colour) in cultured cells (Figure 6 A-D, first row). Curcumin-loaded micelles showed an increase in cell fluorescence intensity associated with curcumin from 6 to 24 h of incubation (Figure 6 E-H, first row). These results indicate that polycaprolactone-grafted oligocarrageenan micelles facilitated the uptake of curcumin into the endothelial cells. Fluorescence quantification confirmed these observations by showing a significant enhancement of encapsulated-curcumin incorporation

inside cells compared to free curcumin (Figure S7). As described by by Sahay, Alakhova, & Kabanov (2008), endocytosis is the main mechanism involved in the internalization of nanometric-sized particles by cells. Polymeric micelles can be taken up by cells using specific mechanisms such as clathrin- or caveolae-mediated endocytosis. Furthermore, Bartczak et al. (2012) showed that spherical particles achieved the highest cellular uptake by human endothelial cells compared to other shapes, such as rod shapes or hollow particles. Further study will help to determine the endocytosis pathway implicated in the uptake of our micelles.

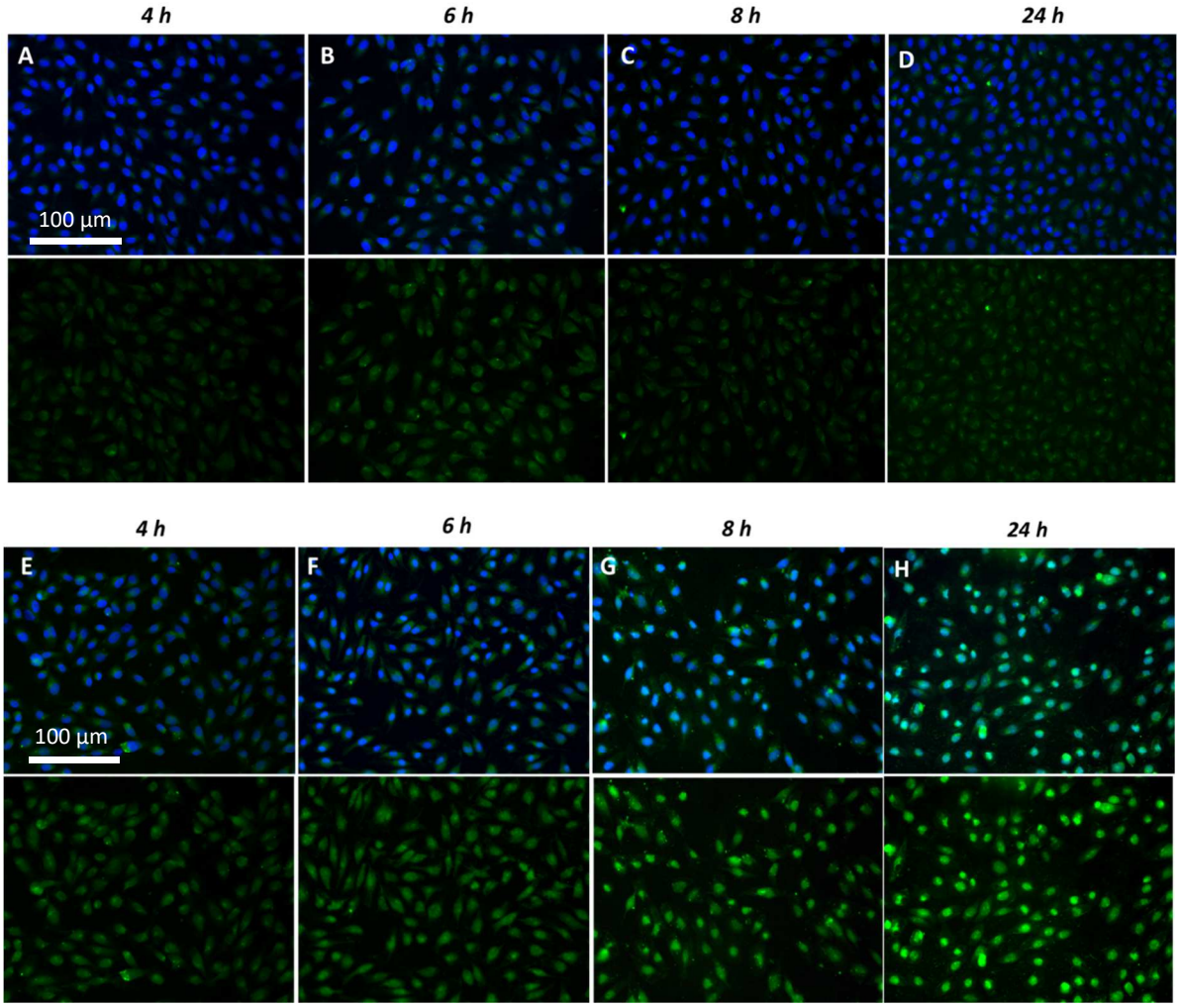

Figure 6: EA.h926 cellular uptake of free curcumin (**A-D**) and curcumin-loaded micelles (**E-H**). The incorporation was studied between 4 h and 24 h with free or encapsulated curcumin at 15 µM. For each condition, the overlay of DAPI staining (blue, nuclear) with curcumin fluorescence (green) is shown in the first row and curcumin fluorescence only in the second row.

3.5. Effect of curcumin-loaded polycaprolactone-grafted oligocarrageenan on inflammation

TNF-alpha was added to the endothelial cells to mimic inflammatory conditions. TNF-alpha induces the secretion of inflammatory factors such as IL-6 and MCP-1 (Scarpini et al., 1999; Cella, Engering, Pinet, Pieters, & Lanzavecchia, 1997). The effects of free curcumin and curcumin-loaded OligoKC-g-PCL were investigated on endothelial cells in inflammatory conditions. Empty polycaprolactone-grafted oligocarrageenan was used as control. Free or encapsulated curcumin at 5 µM did not modify the secretion of IL-6. At a higher dose of 15 µM, the encapsulated curcumin inhibited almost completely the TNF-induced IL-6 production, while the free curcumin induced no significant effect compared to control (Figure 7A). For the chemokine MCP-1, the dose of 5 µM of free or encapsulated curcumin had a similar inhibitory effect. The 15 µM concentration induced a greater inhibition for the encapsulated curcumin relative to free curcumin, reaching levels similar to those of non-stimulated cells (Figure 7B). The inhibitory effect of curcumin on TNF-alpha-stimulated cells was thus significantly enhanced when curcumin was encapsulated into polycaprolactone-grafted oligocarrageenan which is associated with its enhanced cellular uptake.

These results are in agreement with other studies using vectorized curcumin. Liposome-loaded curcumin induced a reduction in IL-1β and TNF-α secretion by lipopolysaccharide (LPS)-stimulated macrophages, compared to free curcumin (Basnet, Hussain, Tho, & Skalko-Basnet, 2012). In another study performed in LPS-injected mice, curcumin-loaded exosomes showed better anti-inflammatory effects than free curcumin (Sun et al., 2010).

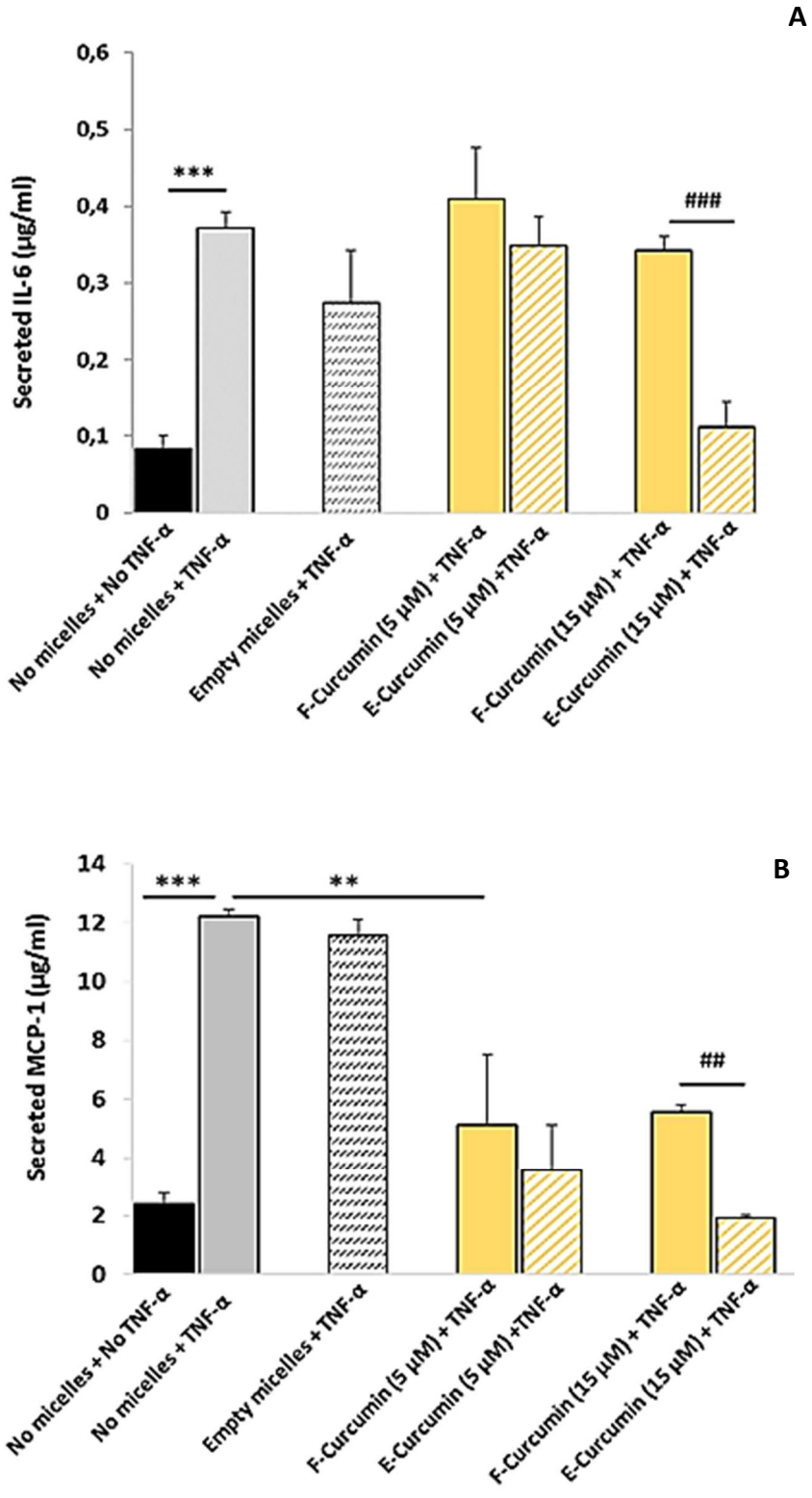

Figure 7: Effect of free curcumin (F-curcumin) and encapsulated curcumin (E-curcumin) on the production of IL-6 (**A**) and MCP-1 (**B**) by EA.h926 stimulated by TNF-alpha. Cells were treated for 24 h with free or encapsulated curcumin at 5 µM and 15 µM and then stimulated by TNF-α (10 ng/mL) overnight. *$p < 0.05$, **$p < 0.01$, ***$p < 0.001$ compared to TNF-α stimulated group without micelles (No micelles + TNF-α) and $^{\#\#}p < 0.01$ compared to cells treated with Free-curcumin at 15 µM.

3.6 Biodistribution in mouse

An *in vivo* biodistribution study was performed using micelles loaded with Nile red (100 mg/kg equivalent to 225 µg of Nile red), due to its greater fluorescence intensity and less complex metabolization than curcumin. The micelles were injected into C57/Bl6 mice.

The plasma concentration of Nile red was measured at 1 h, 2 h and 4 h after injection. As shown in Figure 8A, free Nile red gave higher levels in the blood than did encapsulated Nile red. At 1 h, free Nile red concentration was 2.3-fold higher than micelle-loaded-Nile red. This difference was exacerbated between 1 and 2 hours after injection. At 4 h, both free and encapsulated Nile red had been completely cleared from the blood (distributed into organs or eliminated from the body).

Biodistribution of free Nile red and encapsulated Nile red in various organs was then studied in these mice. For this, tissue homogenates were prepared for liver, brain, kidneys, spleen, and adipose tissue, 4 h after injection. The maximal concentration of Nile red was observed in the liver which is the principal organ involved in the metabolism of exogenous molecules (Figure 8B). In the other organs, fluorescence intensity was comparatively weak, but results showed that micelles improved the incorporation of Nile red into the brain and the lung. In the adipose tissue, only free Nile red was detected, probably due to its lipophilic nature. It is interesting to note that scientific reports demonstrate that curcumin has a high therapeutic ability for treating hepatic disorders (Nabavi, Daglia, Moghaddam, Habtemariam, & Nabavi, 2014).

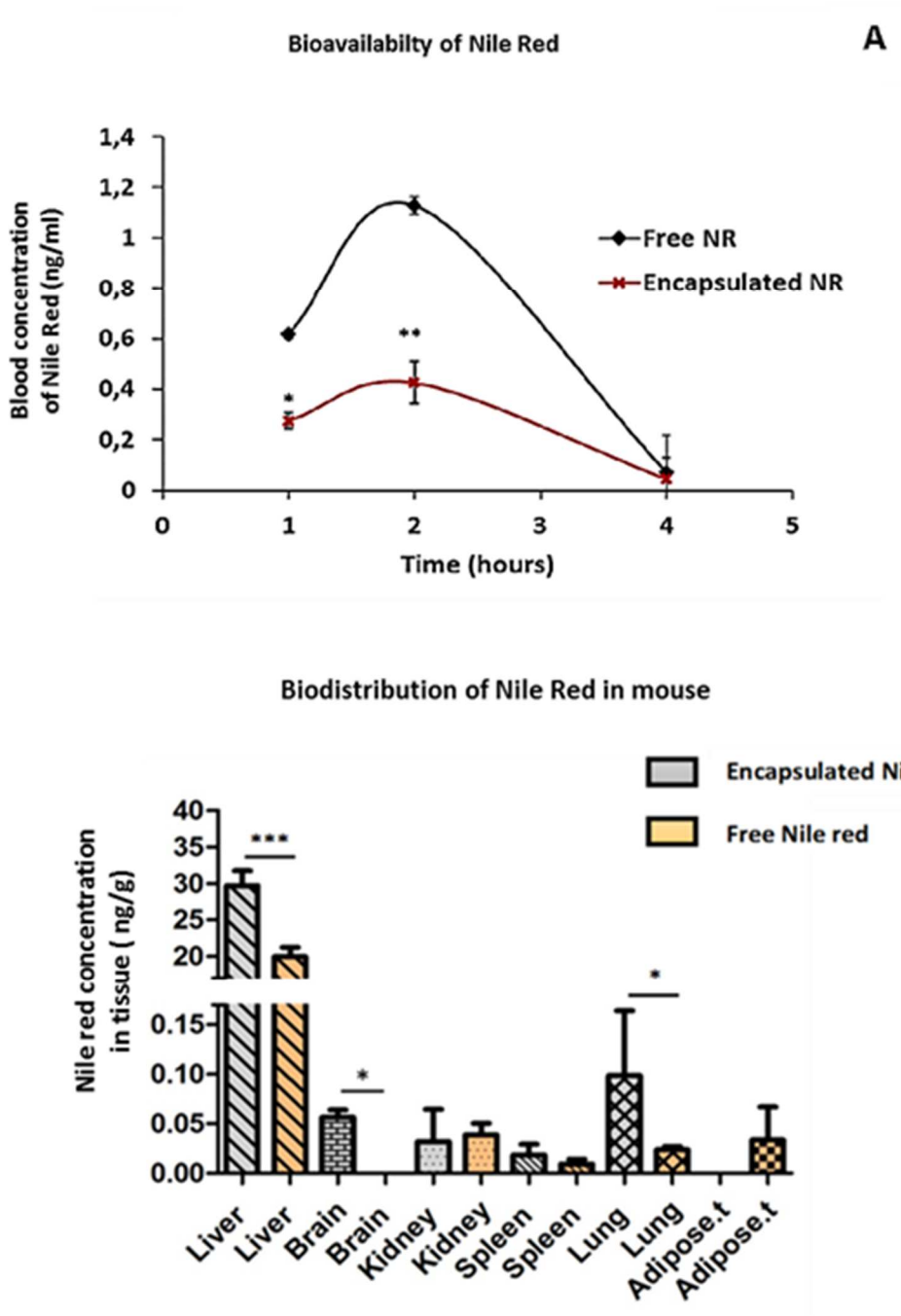

Figure 8: Biodistribution of free and encapsulated Nile red in C57/Bl6 mice studied after intravenous injection. To measure the bioavailability of Nile Red, retro-orbital sampling was performed at 1h, 2h and 4h. Nile red was then extracted from the blood and quantified by fluorescence (**A**). Mice were sacrificed after 4h and Nile red in organs extracted and quantified to study the biodistribution (**B**). Excitation of Nile Red was performed at 550 nm and emission was observed at 630 nm. Both experiments were performed in triplicate (n=3).

4. Conclusion

Oligocarrageenans (DP=8) produced by selective enzymatic hydrolysis of carrageenans were successfully functionalized via grafting of polycaprolactone chains. The graft copolymer

self-assembled into spherical nanomicelles of diameter in the range of 150-200 nm. Hydrophobic molecules were successfully encapsulated and released in a sustained manner. Empty polycaprolactone-grafted oligocarrageenan micelles were not cytotoxic to zebrafish or endothelial cells and they increased the delivery of curcumin into the cells as evidenced by fluorescence microscopy. The nanomicelles also potentiate the anti-inflammatory activity of curcumin in TNF-stimulated endothelial cells as demonstrated by the decreased secreted levels of inflammatory factors IL-6 and MCP-1.

Our *in vivo* study showed that the nanomicelles improved the distribution of Nile red to organs. In particular, the nanomicelles enhanced the incorporation of this hydrophobic molecule into the liver but also the brain. This suggests that polycaprolactone-grafted oligocarrageenan could promote the delivery of hydrophobic therapeutic molecules across the blood-brain barrier ~~(BBB)~~. Further studies are required to determine the mechanisms for the delivery of encapsulated molecules to the brain parenchyma.

These first *in vivo* experiments are promising and now pave the way for further *in vivo* studies. In addition, the presence of free hydroxyl groups and galactose end groups on the micelles offers the possibility to graft specific sequences like antibodies and thus to target tissues. The ability of the micelles to encapsulate larger molecules, such as rifampicin, also opens up the possibility of dual molecule encapsulation.

Supporting Information, SI

Figure S1: Chemical structure of the three main classes of κ-carrageenan and curcumin.

Figure S2: ^{1}H and ^{13}C NMR spectra of curcumin.

Figure S3: HPLC analysis of curcumin.

Figure S4: Determination of CMC (critical micelle concentration) of oligocarrageenan-g-PCL by dynamic light scattering.

Figure S5: Hydrolysis of κ-carrageenan using κ-carrageenase isolated from *Pseudoaltermonas carrageenovora*.

Figure S6: 600 MHz NMR COSY, ^{1}H-^{13}C HSQC and 1D ^{13}C spectra of oligocarrageenan-graft-PCL recorded in D_2O at 25 °C.

Figure S7: Fluorescence quantification of free (F-curcumin) or encapsulated-curcumin (E-curcumin) incorporated in Eahy926 endothelial cells between 4 and 24 h.

Acknowledgements

The authors would like to thank the department of Mayotte, the Regional Council, the BioST federation from University of La Réunion, the FEDER and the Mauritius Research Council for their financial support. Experiments were carried out in DéTROI unit at the CYROI biotechnologies platform (La Réunion) and at the CBBR (Mauritius). Members of DéTROI and CBBR teams are gratefully acknowledged. TEM experiments were performed at the TEM-SEM microscopy platform of the "Institut des Matériaux Paris Centre (IMPC)" of the Sorbonne University, Paris. The authors thank Dr Mary Osborne-Pellegrin for help in editing the manuscript.

References

Barahona, T.; Chandía, N. P.; Encinas, M.; Matsuhiro, B.; Zúñiga, E. Antioxidant capacity of sulfated polysaccharides from seaweeds. A kinetic approach. *Food Hydrocolloid* **2011**, *25*, 529-535, DOI: 10.1016/j.foodhyd.2010.08.004

Bartczak, D.; Muskens, O. L.; Nitti, S.; Sanchez-Elsner, T.; Millar, T. M.; Kanaras, A.G. Interactions of human endothelial cells with gold nanoparticles of different morphologies. *Small* **2012**, *8*, 122-130, DOI: 10.1002/smll.201101422

Basnet, P.; Hussain, H.; Tho, I.; Skalko-Basnet, N. Liposomal delivery system enhances anti-inflammatory properties of curcumin. *J. Pharm. Sci.* **2012**, *101*, 598-609, DOI: 10.1002/jps.22785

Bhaw-Luximon, A.; Jhurry, D.; Booluck, M. H.; Correc, G.; Génicot, S.; Helbert, W. Oligoagarose-graft-polycaprolactone copolymers: synthesis and characterization. *Macromol. Symp.* **2009**, *277*, 14-23, DOI: 10.1002/masy.200950303

Bhaw-Luximon, A.; Meeram, L. M.; Jugdawa, Y.; Helbert, W.; Jhurry, D. Oligoagarose-g-polycaprolactone loaded nanoparticles for drug delivery applications. *Polym. Chem*. **2011**, *2*, 77-79, DOI: 10.1039/C0PY00311E

Boopathy, N; Kandasamy, K. Anticancer drugs from marine Flora: An Overview. *J. Oncol.* **2010**, 214186, 1-18, DOI: 10.1155/2010/214186

Bordallo, E.; Rieumont, J.; Tiera, M. J. ; Gómez, M.; Lazzari, M. Self-assembly in aqueous solution of amphiphilic graft copolymers from oxidized carboxymethylcellulose. *Carbohydr Polym.* **2015**, *124*, 43-49, DOI: 10.1016/j.carbpol.2015.01.082

Bouhlal, R.; Haslin, C.; Chermann, J. C.; Colliec-Jouault, S.; Sinquin, C.; Simon, G.; Cerantola, S.; Riadi, H.; Bourgougnon, N. Antiviral activities of sulfated polysaccharides isolated from Sphaerococcus coronopifolius (rhodophytha, gigartinales) and Boergeseniella thuyoides (rhodophyta, ceramiales). *Mar. Drugs* **2011**, *9*, 1187-1209, DOI: 10.3390/md9071187

716 Cardoso, S. M.; Pereira, O. R.; Seca, A. M. L.; Pinto, D. C. G. A.; Silva, A. M. S. Seaweeds
717 as preventive agents for cardiovascular diseases: from nutrients to functional foods. *Mar.*
718 *Drugs* **2015**, *13*, 6838-6865, DOI: 10.3390/md13116838
719
720 Cavalli, R.; Leone, F.; Minelli, R.; Fantozzi, R.; Dianzani, C. New chitosan nanospheres for
721 the delivery of 5-fluorouracil: preparation, characterization and *in vitro* studies. *Curr. Drug*
722 *Deliv.* **2014**, *11*, 270-278
723
724 Cella, M.; Engering, A.; Pinet, V.; Pieters, J.; Lanzavecchia, A. Inflammatory stimuli induce
725 accumulation of MHC class II complexes on dendritic cells. *Nature* **1997**, *388,* 782-787, DOI:
726 10.1038/42030
727
728 Ciancia, M.; Quintana, I.; Cerezo, A. S. Overview of anticoagulant activity of sulfated
729 polysaccharides from seaweeds in relation to their structures, focusing on those of green
730 seaweeds. *Curr. Med. Chem.* **2010**, *17*, 2503-2529, DOI: 10.2174/092986710791556069
731
732 Cook, M. T.; Tzortzis, G.; Charalampopoulos, D.; Khutoryanskiy, V. V. Production and
733 evaluation of dry alginate-chitosan microcapsules as an enteric delivery vehicle for probiotic
734 bacteria. *Biomacromolecules* **2011**, *12*, 2834-2840, DOI: 10.1021/bm200576h
735
736 Cumashi, A; Ushakova, N.-A.; Preobrazhenskaya, M. E.; D'Incecco, A.; Piccoli, A.; Totani,
737 L; Tinari, N.; Morozevich, G. E.; Berman, A.E.; Bilan, M. I.; Usov, A. I.; Ustyuzhanina, N.
738 E.; Grachev, A.A.; Sanderson, C. J.; Kelly, M.; Rabinovich, G.A.; Iacobelli, S.; Nifantiev, N.
739 E. A comparative study of the anti-inflammatory, anticoagulant, antiangiogenic, and
740 antiadhesive activities of nine different fucoidans from brown seaweeds. *Glycobiology* **2007**,
741 *17*, 541-552, DOI: 10.1093/glycob/cwm014
742
743 Cunha, L.; Grenha, A. Sulfated seaweed polysaccharides as multifunctional materials in drug
744 delivery applications. *Mar. Drugs* **2016**, 14, 1-41, DOI: 10.3390/md14030042
745
746 Gu, C.; Le, V.; Lang, M.; Liu, J. Preparation of polysaccharide derivates chitosan-graft-
747 poly(ε-caprolactone) amphiphilic copolymer micelles for 5-fluorouracil drug delivery.
748 *Colloids Surf B Biointerfaces* **2014**, *116*, 745-750, DOI: 10.1016/j.colsurfb.2014.01.026
749
750 Guibet, M.; Colin, S.; Barbeyron, T.; Genicot, S.; Kloareg, B.; Michel, G.; Helbert, W.
751 Degradation of λ-carrageenan by Pseudoalteromonas carrageenovora λ-carrageenase: a new
752 family of glycoside hydrolases unrelated to κ- and ι-carrageenases. *Biochem. J.* **2007***, 404*,
753 105-114, DOI: 10.1042//BJ20061359
754
755 He, Y.; Yue, Y.; Zheng, X.; Zhang, K.; Chen, S.; Du, Z. Curcumin, inflammation, and chronic
756 diseases: how are they linked? *Molecules* **2015**, *20*, 9183-9213, DOI:
757 10.3390/molecules20059183
758
759 Heger, M.; van Golen, R. F.; Broekgaarden, M.; Michel, M. C. The molecular basis for the
760 pharmacokinetics and pharmacodynamics of curcumin and its metabolites in relation to
761 cancer. *Pharmacol Rev.* 2013, *66*, 222-307, DOI: 10.1124/pr.110.004044
762
763 Hill, A. J.; Teraoka, H.; Heideman, W.; Peterson, R. E. Zebrafish as a model vertebrate for
764 investigating chemical toxicity. *Toxicol. Sci.* **2005**, *86*, 6-19, DOI: 10.1093/toxsci/kfi110

765
766 Hu, Y.; Jiang, Z.; Chen, R.; Wu, W.; Jiang, X. Degradation and degradation-induced re-
767 assembly of PVP-PCL micelles. *Biomacromolecules* **2010**, *11*, 481-488, DOI:
768 10.1021/bm901211r
769
770 Jeetah, R.; Bhaw-Luximon, A.; Jhurry, D. Dual Encapsulation and controlled delivery of anti-
771 TB drugs from PEG-block-poly(ester-ether) nanomicelles. *J. Nanopharmaceutics Drug Deliv.*
772 **2013**, *1*, 240-257, DOI: 10.1166/jnd.2013.1025
773
774 Kam, A.; Li, K. M.; Razmovski-Naumovski, V.; Nammi, S.; Chan, K.; Grau, G. E..; Li, G. Q.
775 Curcumin reduces tumour necrosis factor-enhanced Annexin V-Positive Microparticle
776 Release in Human Vascular Endothelial Cells. *J. Pharm. Pharm. Sci.* **2015**, *18*, 424-433,
777 DOI: 10.18433/J3ZC8G
778
779 Kidby, D. K.; Davidson, D. J. A convenient ferricyanide estimation of reducing sugars in the
780 nanomole range. *Anal. Biochem.* **1973**, *55*, 321-325, DOI: 10.1016/0003-2697(73)90323-0
781
782 Kim, T. H.; Jiang, H. H.; Youn, Y. S.; Park, C. W.; Tak, K. K.; Lee, S.; Kim, H.; Jon, S.;
783 Chen, X.; Lee, K. C. Preparation and characterization of water-soluble albumin-bound
784 curcumin nanoparticles with improved antitumor activity, *Int. J. Pharm.* **2011**, *403*, 285-291,
785 DOI: 10.1016/j.ijpharm.2010.10.041
786
787 Knutsen, S. H.; Sletmoen, M.; Kristensen, T.; Barbeyron, T.; Kloareg, B.; Potin, P. A rapid
788 method for the separation and analysis of carrageenan oligosaccharides released by iota- and
789 kappa-carrageenase. *Carbohydr. Res.* **2001**, *331*, 101-106, DOI: 10.1016/S0008-
790 6215(00)00324-4
791
792 Mahmood, K.; Zia, K. M., Zuber, M.; Salman, M.; Anjum, M. N. Recent developments in
793 curcumin and curcumin based polymeric materials for biomedical applications: A review. *Int.*
794 *J. Biol. Macromol.* **2015**, *81*, 877-90, DOI: 10.1016/j.ijbiomac.2015.09.026
795
796 Nabavi, S. F.; Daglia, M.; Moghaddam, A. H.; Habtemariam, S.; Nabavi, S. M. Curcumin and
797 liver disease: from chemistry to medicine. *Compr. Rev. Food Sci. Food Saf.* **2014**, *13*, 62-77,
798 DOI: 10.1111/1541-4337.12047
799
800 Nesamony, J.; Singh, P. R.; Nada, S. E.; Shah, Z. A.; Kolling W. M. Calcium alginate
801 nanoparticles synthesized through a novel interfacial cross-linking method as a potential
802 protein drug delivery system. *J. Pharm. Sci.* **2012**, *101*, 2177-2184, DOI: 10.1002/jps.23104
803
804 Nishimura, Y.; Inoue, A.; Sasagawa, S.; Koiwa, J.; Kawaguchi, K.; Kawase, R.; Maruyama,
805 T.; Kim, S.; Tanaka, T. Using zebrafish in systems toxicology for developmental toxicity
806 testing, *Congenit. Anom.* **2016**, *56*, 18-27, DOI: 10.1111/cga.12142
807
808 Pedersen, U.; Rasmussen, P. B.; Lawesson, S.-O. Synthesis of naturally occurring
809 curcuminoids and related compounds. *Eur. J. Org. Chem.* **1985**, 1557-1569, DOI:
810 10.1002/jlac.198519850805
811
812 Sahay, G; Alakhova, D. Y.; Kabanov, A. V. Endocytosis of nanomedicines. *J Control*
813 *Release.* **2010**, *145*, 182-195, DOI: 10.1016/j.jconrel.2010.01.036

Sang, V. T.; Ngo, D.-H.; Kim, S.-J. Potential targets for anti-inflammatory and anti-allergic activities of marine algae: an overview. *Inflamm. Allergy Drug Targets* **2012**, *11*, 90-101, DOI: 10.2174/187152812800392797

Savjani, K. T.; Gajjar, A. K.; Savjani, J. K. Drug solubility: importance and enhancement techniques. *ISRN Pharm.* **2012**, 1-10, DOI: 10.5402/2012/195727

Scarpini , E.; Conti, G. C.; Bussini, S.; Clerici, R.; Siglienti, I.; Piccio, L.; De Pol, A.; Baron, P. L.; Scarlato, G. Human Schwann Cell Proliferation and IL-6 Production following TNF-alpha Stimulation *in vitro*. *Ann. N. Y. Acad. Sci.* **1999**, *883*, 520-522, DOI: 10.1111/j.1749-6632.1999.tb08626.x

Shakeel, F.; Ramadan, W.; Shafiq, S. Solubility and dissolution improvement of aceclofenac using different nanocarriers. *J. Bioequivalence Bioavailab.* **2009**, *1*, 39-43, DOI: 10.4172/jbb.1000007

Shukla, A.; Ray B.; Maiti P. Grafted cyclodextrin as carrier for control drug delivery and efficient cell killing. *J Biomed Mater Res A.* **2019**, *107*, 434–444, DOI: 10.1002/jbm.a.36560

Sun, D.; Zhuang, X.; Xiang, X.; Liu, Y.; Zhang, S.; Liu, C.; Barnes, S.; Grizzle, W.; Miller, D.; Zhang, H. G. A Novel Nanoparticle Drug Delivery System: The Anti-inflammatory activity of curcumin is enhanced when encapsulated in exosomes, *Mol. Ther.* **2010**, *18*, 1606-1614, DOI: 10.1038/mt.2010.105

Sun, Y.; Liu, Y.; Jiang, K.; Wang, C.; Wang, Z.; Huang, L. Electrospray Ionization Mass Spectrometric Analysis of κ-carrageenan oligosaccharides obtained by degradation with κ-carrageenase from pedobacter hainanensis. *J. Agric. Food Chem.* **2014**, *62*, 2398-2405, DOI: 10.1021/jf500429r

Thiyagarajan, M.; Sharma, S. S. Neuroprotective effect of curcumin in middle cerebral artery occlusion induced focal cerebral ischemia in rats. *Life Sci.* **2004**, *74*, 969-985, DOI: 10.1016/j.lfs.2003.06.042

Topel, Ö.; Cakir, B. A.; Budama, L.; Hoda, N. Determination of critical micelle concentration of polybutadiene-block-poly(ethyleneoxide) diblock copolymer by fluorescence spectroscopy and dynamic light scattering. *J. Mol. Liq.* **2013**, *177*, 40-43, DOI: 10.1016/j.molliq.2012.10.013

Venkatesan, J.; Lowe, B.; Anil, S.; Manivasagan, P.; Al Kheraif, A. A.; Kang, K-. H.; Kim, S-. K. Seaweed polysaccharides and their potential biomedical applications. *Starch Stärke* 2015, *66*, 1–10, DOI: 10.1002/star.201400127

Wang, Z.; Zhao, Y.; Jiang, Y.; Lv, W.; Wu, L.; Wang, B.; Lv, L.; Xu, Q.; Xin, H. Enhanced anti-ischemic stroke of ZL006 by T7-conjugated PEGylated liposomes drug delivery system. *Sci Rep.* **2015**, 5, 12651, DOI: 10.1038/srep12651

Xu, W.; Ling, P.; Zhang, T. Polymeric micelles, a promising drug delivery system to enhance bioavailability of poorly water-soluble drugs. *J. Drug Deliv.* **2013**, 340315, DOI: 10.1155/2013/340315

Yao, Z.; Wang, F.; Gao, Z.; Jin, L.; Wu, H. Characterization of a κ-carrageenase from marine Cellulophaga lytica strain N5-2 and analysis of its degradation products. *Int. J. Mol. Sci.* **2013**, *14*, 24592-24602, DOI: 10.3390/ijms141224592

Youssouf, L; Lallemand, L.; Giraud, P.; Soulé, F.; Bhaw-Luximon, A.; Meilhac, O.; D'Hellencourt, C.L.; Jhurry, D.; Couprie, J. Ultrasound-assisted extraction and structural characterization by NMR of alginates and carrageenans from seaweeds. *Carbohydr. Polym.* **2017**, *166*, 55-63, DOI: 10.1016/j.carbpol.2017.01.041